

## Transient conductivity and photoconductivity in *a*-Si:H

R. A. Street

Xerox Corporation, Palo Alto Research Center, Palo Alto, California 94304

(Received 21 January 1985)

Transient conductivity and photoconductivity are explored in amorphous silicon (*a*-Si:H). The breakdown of the time-of-flight method is demonstrated in doped samples of sufficient bulk conductivity. The transient response is then shown to contain no information about the drift mobility or carrier lifetimes, but instead is governed by the contact depletion-layer capacitance and the bulk series resistance. Analysis of the results gives a new method of determining the density of shallow occupied states in *a*-Si:H and quantitative results are given for some *n*- and *p*-type samples. Measurements of gap-cell photoconductivity are shown to have similar contact effects which causes a decay artifact that can extend up to  $\sim 1$  sec. It is argued that the artifact may have been mistakenly interpreted as bulk dispersive transport and recombination in some published data.

### I. INTRODUCTION

Transient photoconductivity is a powerful technique for exploring transport and recombination in amorphous semiconductors. The concept of dispersive carrier mobility was first demonstrated using this type of experiment,<sup>1</sup> and recently its use with hydrogenated amorphous silicon has been extended to study deep trapping lifetimes,<sup>2-4</sup> transport mechanisms,<sup>5,6</sup> the density of gap states,<sup>7,8</sup> depletion-layer field profiles,<sup>9,10</sup> surface band bending,<sup>11</sup> and interface states.<sup>11,12</sup>

There are two types of sample structure on which transient-photoconductivity measurements are usually made. One of these is a parallel-plate capacitor (sandwich) structure, and the experiment is generally referred to as time of flight (TOF). The alternative is to use a gap cell in which the electrodes are coplanar with a spacing that is much larger than the sample thickness.

In the usual TOF experiment the observed photocurrent  $I(t)$  during the carrier transit is described by

$$I(t) = ne\mu E, \quad (1)$$

where  $n$  is the carrier density and  $\mu$  the drift mobility, and it is assumed that the field  $E = V/d$  is uniform in the sample. It has long been recognized that special precautions are necessary to ensure that  $E$  is indeed uniform. Usually a pulsed field is applied such that the time between the voltage pulse and the illumination is as short as possible. This delay time must be shorter than the dielectric relaxation time  $\epsilon\epsilon_0\rho_B$ , where  $\rho_B$  is the bulk resistivity, so that in practice the measurement is restricted to low-conductivity samples. In addition blocking contacts are required to prevent large injection currents. All of the usual evaporated metal contacts on *a*-Si:H are sufficiently blocking to satisfy this requirement. Finally, low illumination levels are required so that the transport itself does not distort the field. The appropriate condition is that the transported charge is much less than  $CV$ , where  $C$  is the sample capacitance.

None of these precautions can prevent the effects of an

internal field that is present before the voltage pulse is applied. Such a field is almost unavoidable since the requirement of a blocking contact involves a depletion layer in the semiconductor, and hence an internal field. In *a*-Si:H a significant field often extends about  $1 \mu\text{m}$  from the contact.<sup>9</sup> Hence, although the effect cannot be eliminated, it can be minimized by using sufficiently thick samples.

Although it is necessary to have a uniform field to measure  $\mu$  or  $\mu\tau$ , it is of interest to understand the transient behavior under conditions in which the field is not uniform. In particular this is achieved by applying a constant rather than pulsed voltage, or in measurements on highly conducting samples or on those with injecting contacts. Some of these situations have been explored in recent papers.<sup>9,11</sup> Section III of this paper expands on the properties of these experimental arrangements, and presents new data on doped *a*-Si:H samples. Along with the transient-photoconductivity measurements, pulsed dark-conductivity data are presented, in which the sweep out of carriers is observed.

The principal advantage of using gap-cell structures for transient photoconductivity is that the transport can be measured to long times without encountering transit-time effects. Various groups have observed that the photocurrent has a power-law decay extending over a very wide time range, particularly in *n*-type *a*-Si:H, but also in undoped material.<sup>6,8,13,14</sup> The decay has been interpreted as dispersive transport and bulk recombination, based on Eq. (1). However, the gap-cell experiment is performed under conditions that invalidate the uniform-field assumption used in TOF. In general, the voltage is not applied as a pulse; the transient decay often covers times larger than the dielectric relaxation time of the sample; and the amount of charge transported is much greater than  $CV$ . For the gap-cell measurement it is generally assumed that the sample is a perfect resistor, whereas for TOF it is a perfect capacitor. Hence the standard analysis of photoconductivity<sup>15</sup> assumes ideal Ohmic contacts, whereas in practice, blocking contacts are actually used on *a*-Si:H. Section IV presents transient-photoconductivity-decay

data and uses the information obtained from sandwich structures to clarify the extent to which the approximations used for gap cells are valid.

## II. EXPERIMENTAL METHODS

All of the samples used are glow discharge deposited *a*-Si:H, which have been well characterized by a variety of techniques in this laboratory. The metal contacts are evaporated Cr. Sandwich cells are typically 5  $\mu\text{m}$  thick with 3-mm-diam contacts, and gap cells have 0.15- or 1-mm gaps. The excitation source for photoconductivity is a pulsed nitrogen-dye laser combination. Measurements are performed "single shot" meaning that there is at least a 5–10-sec delay between each pulse, and the results are usually averaged over 5–10 transients. Three experimental configurations are used. In each case both the transient current  $I(t)$ , and the integrated charge collection  $Q = \int I(t)dt$  are measured:

(a) The standard TOF experiment in which a voltage pulse is applied first and the light pulse after  $\sim 10$ – $100 \mu\text{sec}$ .

(b) A dc TOF experiment in which a dc voltage is applied instead of a pulse.

(c) Voltage-pulse measurements in which a voltage pulse is applied but no light. The current immediately after turning on the field is measured.

## III. SANDWICH-CELL DATA AND ANALYSIS

A nonuniform field within the sample invalidates the usual TOF conditions, and leads to a distortion of the response. There are several experimental configurations that result in a nonuniform field, and each has its characteristic properties, depending on the type of sample. Three of these configurations are considered in this section.

### A. dc TOF on undoped *a*-Si:H

It is worth reviewing briefly the effects of dc rather than a pulsed voltage on the TOF measurements on undoped samples. The results are described in more detail elsewhere.<sup>9</sup> Figure 1, taken from Ref. 9, shows a comparison of the electron-transient-photocurrent response in the two cases. With a dc bias, the constant photocurrent and well-defined transit time of the standard TOF are replaced by a monotonically decreasing photocurrent. The different time dependence of the transient occurs because the dc applied voltage is dropped near the metal Schottky contact, rather than uniformly through the bulk, as illustrated in Fig. 1. The photocurrent reflects an internal field which decreases approximately exponentially away from the contact. In general the dc voltage also gives a smaller charge collection than the pulsed-voltage TOF experiment because the depletion layer field typically extends only a fraction of the sample thickness.<sup>9</sup> However, the width depends on the density of states in the gap and therefore is very sensitive to the details of the sample deposition. At the end of the depletion layer the field is so small that the carriers are captured by deep traps before moving significantly further.

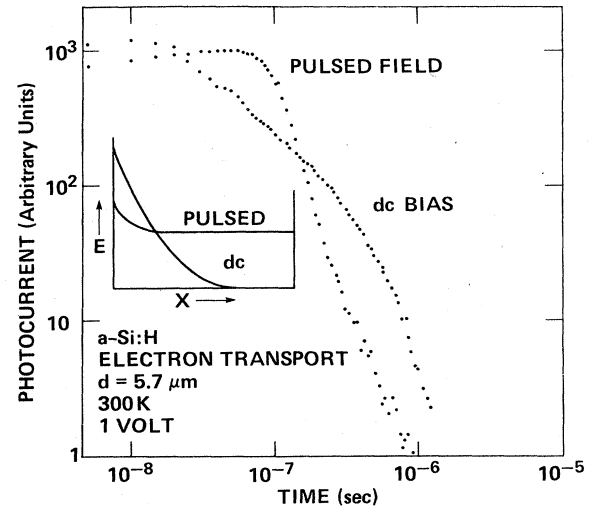


FIG. 1. Comparison of the TOF electron response for pulsed and dc voltages in undoped *a*-Si:H. Also shown is a schematic diagram of the spatial distribution of the internal field in the two cases.

The time to create the equilibrium depletion layer corresponds to the emission time from deep traps,  $w_0^{-1} \exp(E/kT)$ , which is of order 1–10 sec for dangling bonds in *a*-Si:H at 300 K, assuming  $w_0 \sim 10^{12} \text{ sec}^{-1}$  and  $E \sim 0.8 \text{ eV}$ .<sup>16,17</sup> As the space-charge layer is established, carriers emitted from traps are swept out by the field. This is a slow process in undoped samples, and so the current is very low. As we shall see the sweep out is readily observed in doped samples.

This depletion-layer model assumes that the leakage current  $I_L$  across the contact is so small that there is a negligible voltage drop across the sample bulk. The sample can be thought of as a Schottky contact with a series bulk resistance  $R_B$ . The voltage drop across the bulk is therefore  $I_L R_B$ . For example, if the leakage current is  $10^{-8} \text{ A/cm}^2$  and the bulk resistivity is  $10^{10} \Omega \text{ cm}$ , then a sample thickness of 5  $\mu\text{m}$  gives a voltage drop of only 50 mV. Hence under most circumstances the simple model of the depletion layer is valid for undoped *a*-Si:H, and for doped samples the voltage drop in the bulk will be much smaller.

### B. High-conductivity *N*-type *a*-Si:H

The example used to illustrate typical TOF data in conducting *a*-Si:H is an *n*-type sample with a doping level of 1 ppm  $\text{PH}_3/\text{SiH}_4$ . Figure 2 shows examples of the TOF response for both pulsed and dc voltages, corresponding to the transport of electrons. Figure 3 shows the voltage dependence of the charge collection, again for the two types of experiment. Figure 4 shows the results of transient voltage measurements and the charge collection for this mode is given in Fig. 3.

The transients have a number of characteristic properties which are very different from the data on undoped samples.

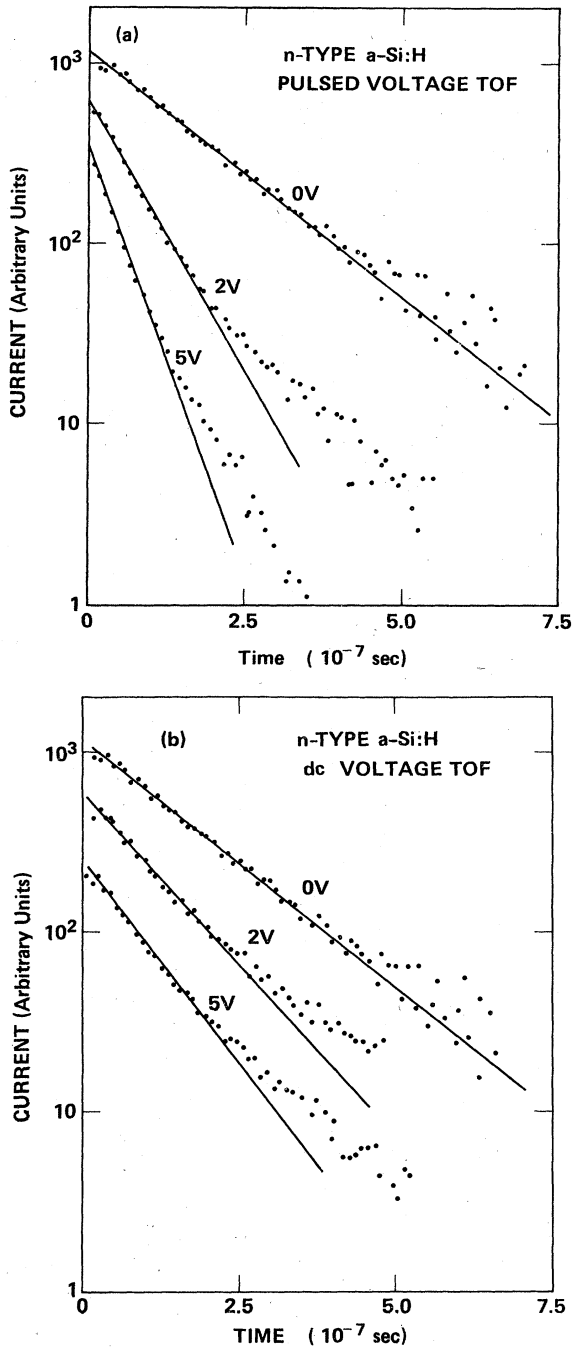


FIG. 2. Comparison of the TOF response for (a) pulsed and (b) dc voltages in the *n*-type sample, showing the voltage dependence of the exponential current decays.

(1) The TOF results do not show an obvious transit time. Instead the response approximates to a simple exponential decay as can be seen from the semilog plots of Fig. 2. Pulsed and dc voltages give different results in that the decay-time constant is smaller for pulsed voltages, with the difference increasing with voltage. (Note,

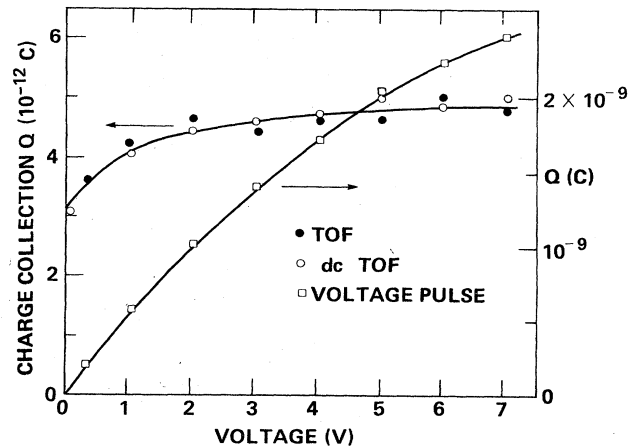


FIG. 3. Charge collection versus voltage for the three types of transient measurements in the *n*-type sample.

in contrast, that in undoped samples the initial decay is faster for the dc bias.)

(2) The charge collection  $Q$  is approximately constant over a wide range of voltages for both types of TOF experiment (Fig. 3), and more significantly the magnitude of  $Q$  demonstrates that essentially full collection of the charge is observed. (The value of  $Q$  corresponding to full collection is calibrated by measurements on undoped samples with identical electrode thickness.)

(3) The voltage-pulse measurements show an extended-time response well beyond the displacement current of the geometrical capacitance as observed in undoped samples (see Fig. 4). Furthermore, this current transient has an exponential decay with a time constant and a voltage depen-

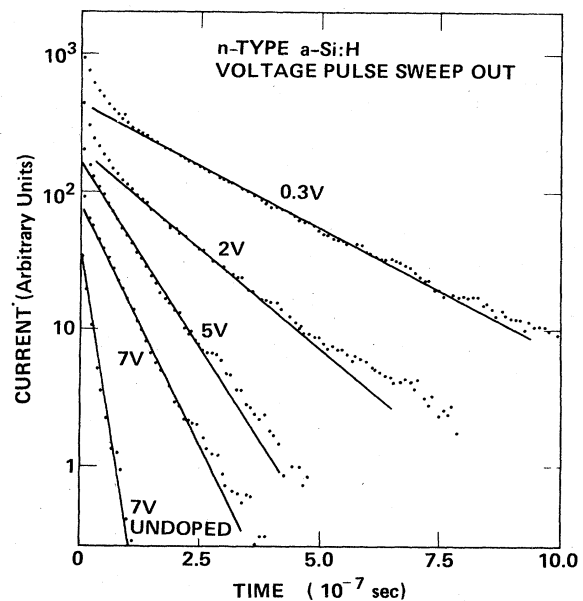


FIG. 4. Examples of the voltage-pulse response for the *n*-type sample. Also shown is the displacement current of an undoped sample.

dence that are very similar to those of the voltage pulse TOF (compare Figs. 2 and 4). Unlike the TOF results, the voltage-pulse charge collection increases with applied voltage (Fig. 3).

The response of this *n*-type sample is in fact easy to understand, and originates from the formation of a depletion layer at the contact coupled with the relatively high bulk conductivity. The sample is characterized as a capacitance  $C$  of the depletion layer in series with a resistance  $R$  of the undepleted bulk (plus any external series resistance). When a voltage is applied, carriers are swept out to form the space-charge layer. Hence the voltage-pulse response approximates to an exponential decay with a time constant equal to  $RC$ . Because the conductivity of *n*-type *a*-Si:H is high, the time constant is  $10^{-7}$  sec compared to the equivalent time of 1–10 sec in undoped samples. The current is correspondingly larger and easily measured.

The fact that the voltage-pulse charge collection increases with voltage (see Fig. 3) demonstrates that the sample is not fully depleted by the voltage pulse. Consequently after the voltage is applied, the internal field extends over only a fraction of the sample thickness. It may therefore seem surprising that the TOF data show full charge collection, indicative of carriers that completely cross the sample. The explanation of this result is that the TOF charge collection in fact contains two components. The first we refer to as the "electrostatic" term, and is the only contribution observed in undoped samples. When the optically excited charge  $q$  moves a distance  $x$ , then a total charge  $qx/d$  is induced on the back contact. However, the motion of this charge generates a small distortion of the field in the sample. In an *n*-type sample, the excited electrons will drift rapidly across the depletion layer and generate a field in the undepleted, highly conducting bulk. As a result, a current will flow until the electron charge is screened out. We refer to this component as the "screening" term, and the sum of the two components can easily be shown to give a total charge collection of  $q$  (i.e., complete collection). It is clear that if  $x/d$  is small, most of the observed charge collection arises from the screening term. Furthermore, the screening process is essentially identical to the sweep out in the voltage-pulse measurement, so that similar  $RC$  time constants are expected. The important conclusion is that the TOF charge collection in doped samples has nothing to do with the actual drift length of the excited carriers, and the response time is unconnected with any bulk transit or trapping time. The same screening term is unobservable in the TOF of undoped samples, because the conductivity is so low that the associated current is unmeasurably small.

It remains to discuss the difference between the pulsed and dc-TOF transients which is a consequence of the distribution of deep and shallow states in *a*-Si:H. The initial sweep out of charge only occurs from shallow states near the Fermi energy, because emission of carriers from deep-dangling bond states is very slow. Hence the pulsed voltage initially forms a depletion layer characteristic of only the shallow-state density, whereas in the dc measurement, the deep states influence, and in fact dominate the

depletion layer. This distinction highlights the main usefulness of the present experiments since, as detailed below, they serve as an effective measure of shallow states.

### C. Analysis

To analyze the results in more detail we use the density-of-states diagram illustrated in Fig. 5. In *n*-type *a*-Si:H, the Fermi energy  $E_F$  is in the conduction-band tail, and these states are separated from the dangling bonds near mid gap by a deep minimum in the density of states.<sup>16,17</sup> For the timescale of the measurements we are considering, only band-tail states respond. Since the conduction-band tail has a characteristic width of the same magnitude as  $kT$  at 300 K, the states near  $E_F$  fall in a relatively narrow energy range, so that the range of thermal excitation times is similar to the average sweep out time. The band of electrons can therefore be considered as a discrete level, which greatly simplifies the analysis. This approximation breaks down for *p*-type samples because the valence band tail is broader, as described below.

The charge swept out during the voltage-pulse experiment is given by

$$Q(V) = neA(x - x_0), \quad (2)$$

where  $n$  is the density of shallow occupied states,  $x_0$  and  $x$  are the depletion-layer widths at zero bias and after the sweep out, and  $A$  is the sample area. The solution to Poisson's equation for a discrete level of states is

$$V - V' = nex^2 / 2\epsilon\epsilon_0, \quad (3)$$

with

$$V' = V_0 - nex_0^2 / 2\epsilon\epsilon_0. \quad (4)$$

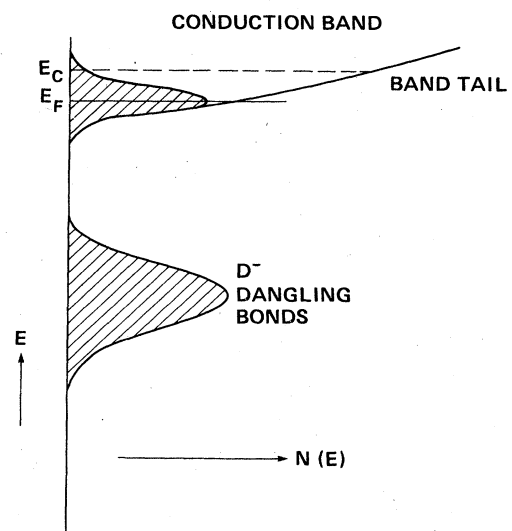


FIG. 5. Schematic density of states diagram for the upper half of the gap showing the clear separation of the shallow and deep states.

Here  $V_0$  is the built-in potential and  $\epsilon\epsilon_0$  is the dielectric constant. This result is slightly different from the usual depletion approximation because  $x_0$  is an equilibrium depletion layer and is determined by all the gap states, whereas  $x$  is only determined by shallow states. Consequently,  $V'$  is not the built-in potential.

Substituting Eqs. (3) and (4) into Eq. (2) gives

$$Q^2(V) = 2\epsilon\epsilon_0 neA^2 \{ (V - V'') - [4(V - V')(V_0 - V')]^{1/2} \}, \quad (5)$$

where  $V'' = 2V' - V_0$ . The density of dangling bonds is known to be much larger than of the shallow occupied tail states. Therefore  $x_0$  is small, and  $V' \simeq V_0$ . Consequently the square-root term on the right-hand side of Eq. (5) is small compared to the term linear in  $V$ , provided  $V$  is measured up to about 10 V. In the following analysis, this term is neglected. As a result the deduced value of  $n$  is underestimated by approximately 10%, although the precise correction depends on the values of  $V_0$  and  $x_0$ , neither of which is accurately known.

Equation (5) is functionally equivalent to the capacitance-voltage relation for a depletion layer, and allows  $n$  to be obtained. Figure 6 shows the charge-collection data of Fig. 3 plotted as  $Q^2$ . A linear fit is obtained and the derived density of states is  $6 \times 10^{14} \text{ cm}^{-3}$  [neglecting the square-root term in Eq. (5)] which agrees well with other measurements of this quantity.<sup>18</sup> For this density of states and the charge collection given in Fig. 6, the predicted depletion-layer width ( $Q/neA$ ) is about 3  $\mu\text{m}$  at the highest measured voltage. Full depletion is expected to occur near 14 V. The linear fit of  $Q^2$  confirms that the depletion approximation is valid and indicates that the band-tail states do indeed form a narrow level. The intercept with the voltage axis is negative, and clearly

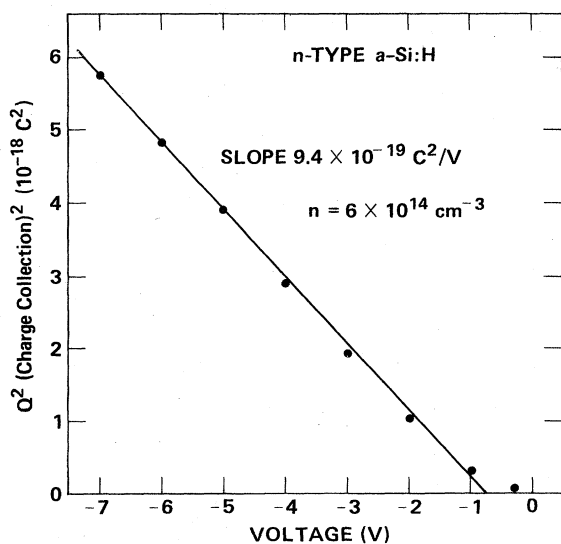


FIG. 6. Plot of charge collection squared versus voltage from voltage-pulse data, giving the density of shallow states as described in the text.

does not correspond to the built-in potential, as is brought out by the analysis.

The calculation of the sweep out current decay is rather complicated, but can be simplified by assuming that the decay is exponential

$$I = I_0 \exp(-t/\tau). \quad (6)$$

The data of Fig. 4 show this to be a reasonable approximation. Hence

$$Q = I_0 \tau = V \tau / R, \quad (7)$$

where  $R$  is the series resistance. Hence substituting for  $Q$  in Eq. (5) gives

$$V - V''' = 2ne\epsilon\epsilon_0 R^2 A^2 / \tau^2, \quad (8)$$

where terms containing the square root of  $V$ , similar to those in Eq. (5), are neglected and  $V''' \neq V''$ .

Equation (8) provides an alternative method of obtaining  $n$ , although since the decay data are usually slightly nonexponential, the results have a larger uncertainty. However, the decay data offer two advantages. One is that Eq. (7) can be used to obtain the bulk resistivity of the sample, without problems from contact effects. The temperature dependence of the resistivity of an  $n$ -type sample is given elsewhere using this technique,<sup>11</sup> and as a check on the validity of the analysis, it is confirmed that  $V\tau/Q = R$  is independent of  $V$ , leading to a consistent value of  $R$ .

The second use of the decay data is to investigate the time-dependent formation of the equilibrium depletion layer, since  $\tau$  can be measured at any time after voltage pulse. Figure 7 shows examples in which  $1/\tau^2$  is plotted for different experimental conditions: as a function of voltage for a delay of 50  $\mu\text{sec}$ , for a dc voltage, and as a function of delay for a fixed voltage. The results are a nice illustration of the initial formation of the depletion layer and its shrinking down to the equilibrium value. The steep slope of the voltage-pulse TOF data is characteristic of the low density of shallow states, and in fact Eq. (8) gives a density of states consistent with the  $Q^2$  data in Fig. 6. The much larger time constants of the dc TOF data in Fig. 7 indicate a reduced depletion layer due to a large space-charge density, as expected, since the density of dangling bonds is much higher than that of shallow occupied states. Furthermore, the transition to the equilibrium state mostly occurs for delay times larger than 1 msec, which is consistent with the emission times of dangling bonds.<sup>16</sup>

To summarize the preceding results, when the  $a\text{-Si:H}$  sample is sufficiently conducting, the TOF data are completely different from those of undoped samples. No bulk transport information is obtained (i.e., the drift mobility or  $\mu\tau$ ). Instead the results can be analyzed to give the density of shallow states and the sample bulk conductivity. The properties we have described for a sample which is not fully depleted of shallow states by a voltage pulse have the following characteristics.

(a) Complete charge collection is observed in both dc and pulsed TOF experiments.

(b) The TOF and the pulsed-voltage response have simi-

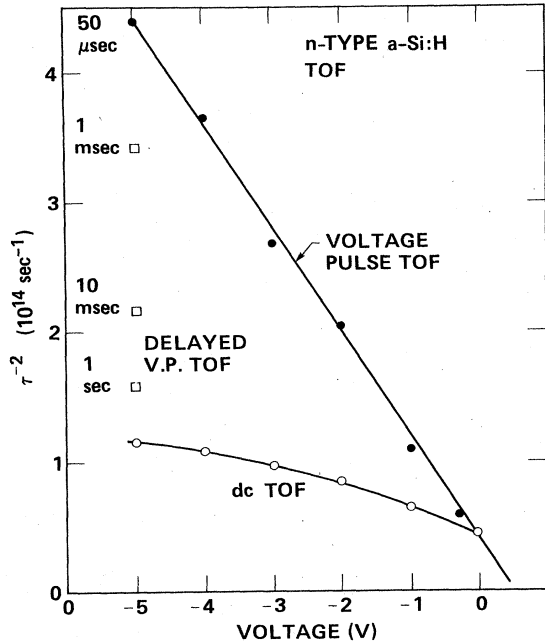


FIG. 7. Plot of inverse time-constant squared versus voltage for normal and dc TOF data, and for variable delay times, indicating the collapse of the depletion layer.

lar exponential decays, with time constants that vary with voltage.

(c) The pulsed-voltage charge collection increases with  $V$ , and is the signature that full depletion is not obtained. The quantity  $V\tau/Q$  is constant and equals the series resistance of the sample.

(d) A plot of  $Q^2$  or  $1/\tau^2$  versus  $V$  gives directly the density of shallow states.

#### D. Intermediate conductivity *p*-type *a*-Si:H

There is an intermediate regime in which both a normal TOF transit time and charge sweep out can be observed. The sample used as an illustration is *p*-type, doped  $10^{-4}$   $\text{B}_2\text{H}_6/\text{SiH}_4$ . Figure 8 shows TOF data which clearly indicate a transit time and dispersive mobility for holes, with results for the mobility and its activation energy that are typical of other hole mobility data.<sup>2,7,19</sup> However, voltage-pulse sweep out is also observed and examples are given in Fig. 9. Initially the sweep-out current drops exponentially, but there is a long slow tail to the decay.

Based on the discussion of the preceding section, it should be impossible to observe a normal transit and to form a hole depletion layer during the sweep out. The only way the two results can occur is if the sample is fully depleted of shallow states even at low voltages. Full depletion means that although there is a space charge, at large voltages the field will be reasonably uniform throughout the bulk, and there are no mobile carriers to give the screening contribution to the charge transport.

If the sample is fully depleted, the sweep-out charge should be independent of voltage. Figure 10 shows that

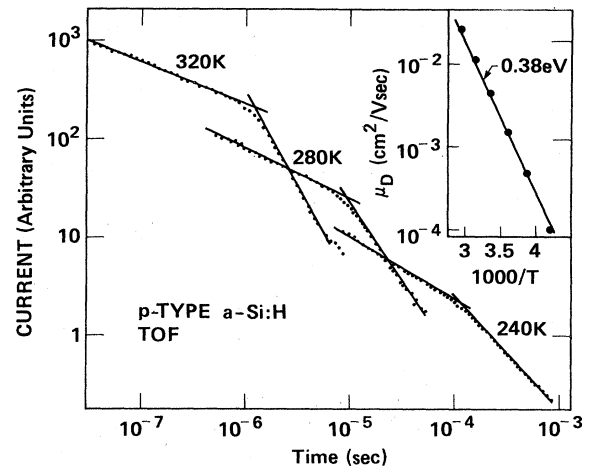


FIG. 8. TOF measurements from the *p*-type sample, showing hole transits at different temperatures. The temperature dependence of the drift mobility is shown in the inset.

indeed  $Q$  is constant above 2 V, in contrast to the result for *n*-type samples (compare Fig. 3). Assuming that the sweep-out current decay is approximately exponential, then from Eq. (7), a constant value of  $Q$  implies  $1/\tau \sim V$ . Again, this behavior is confirmed in Fig. 10, in contrast to the  $1/\tau^2$  versus  $V$  plots obtained in the *n*-type samples.

The condition of full depletion of shallow states is therefore easy to recognize. The density of occupied shallow states can immediately be deduced, being  $2Q/Aed$ , where  $d$  is the sample thickness. From the data in Fig. 10, the density obtained is  $2 \times 10^{14} \text{ cm}^{-3}$ . Application of Eq. (3) shows that for this density of states, full depletion

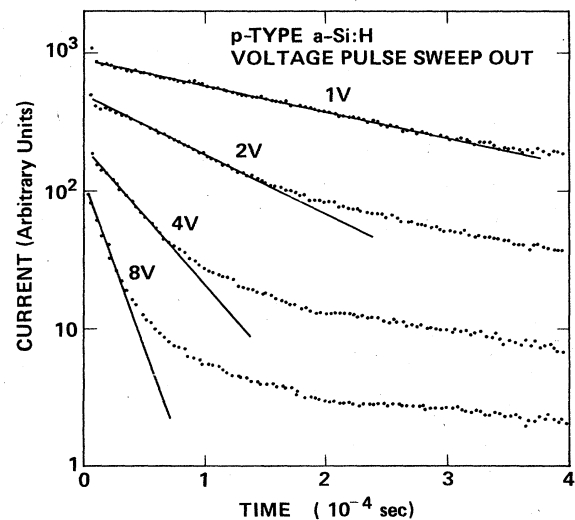


FIG. 9. Examples of the voltage-pulse response for *p*-type *a*-Si:H.

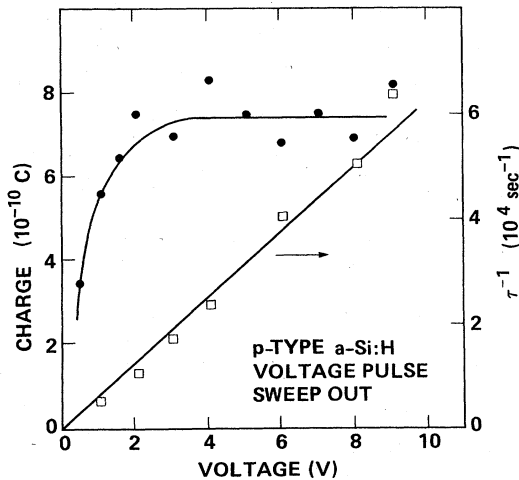


FIG. 10. Charge-collection and inverse decay-time data versus voltage from voltage-pulse measurements for the *p*-type sample.

should occur at 4 V, in good agreement with the observations of Fig. 10. In addition the bulk resistivity can be obtained from measurements of  $V\tau/Q$  as for the *n*-type samples. Figure 11 shows the decay times measured over a range of temperatures. To cope with the nonexponential decay the average time constant is defined as being when a  $\log I$ - $\log t$  plot has a slope of  $-1$ , as was used elsewhere.<sup>11</sup> This definition leads to a time constant that is no more than a factor of 2 different from the initial decay as in Fig. 9, and reduces the possible ambiguity of a tem-

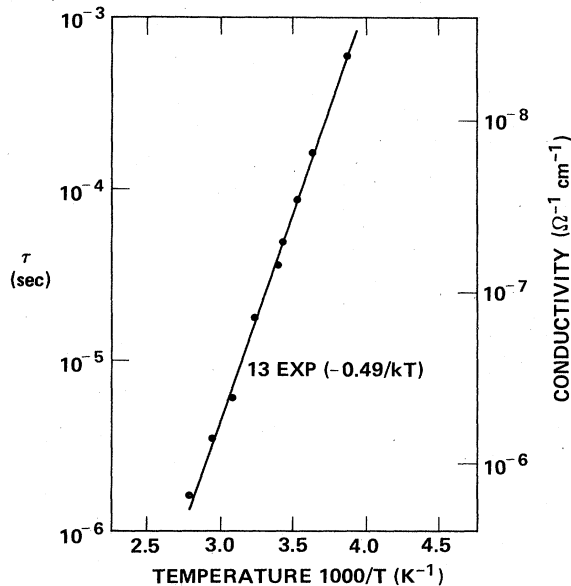


FIG. 11. Temperature dependence of the voltage-pulse decay times for the *p*-type sample, giving the bulk conductivity.

perature dependence in the distribution of time constants. The conductivity is obtained using the known values of  $Q$ ,  $V$ , and the sample geometry, and has an activation energy of 0.5 eV, a room-temperature value of  $5 \times 10^{-8} \Omega^{-1} \text{cm}^{-1}$ , and a prefactor of  $13 \Omega^{-1} \text{cm}^{-1}$ .

The measurement of  $Q$  in the *p*-type sample has a larger uncertainty than in the *n*-type sample because of the extended time response evident in Fig. 9. We attribute the extended decay to the broader band tail, known to be present at the valence-band edge, such that a significant density of holes come from states more than  $kT$  from the Fermi energy. The charge collection in Fig. 10 is measured out to 10 msec, at which time the base-line dominates the measured current. Typically the time range 1–10 msec contributes less than half the total  $Q$ . Based on these observations, the uncertainty in  $Q$  is estimated to be  $\sim 50\%$ . In addition, to the extent that there is a continuous distribution of states, the distinction between shallow and deep states becomes blurred. The range of measurement times, about two decades after the initial decay, corresponds to emission from states spread over  $\sim 0.1$  eV from the Fermi energy.

It is of interest to compare the measured density of states with an exponential band-tail model, in which the density of states is given by

$$N(E) = N_v \exp(-E/E_c). \quad (9)$$

Assuming that the density of states at the mobility edge  $N_v$  is  $10^{21} \text{cm}^{-3} \text{eV}^{-1}$  and that  $E_c$  is 40 meV as indicated by the measurements of dispersive drift mobility, then the total density of occupied states above the Fermi energy is given by  $E_c N(0.5)$  and has a value  $1.5 \times 10^{14} \text{cm}^{-3}$ , which is very close to the measured result. A similar estimate for the conduction band assuming  $E_F$  is at 0.2 eV and  $E_c$  is 20 meV leads to an estimate of  $9 \times 10^{14} \text{cm}^{-3}$ , again close to the measured value for the sample described in Sec. III B. Both results are therefore consistent with exponential band tails extending well into the gap. On the other hand, at a *p*-type doping level of  $10^{-4}$ , it is known that the sample contains  $3 \times 10^{17} \text{cm}^{-3}$  dangling bonds acting as deep states and located near midgap.<sup>20,21</sup> The present experiments therefore suggest that there is a deep minimum in the density of states above the valence-band tail in boron-doped *a*-Si:H, just as has been found below the conduction-band tail in *n*-type *a*-SiH,<sup>17</sup> and that in the minimum the density of states is no more than  $3 \times 10^{15} \text{cm}^{-3} \text{eV}^{-1}$ . Other data seem to indicate a much larger density of states in boron-doped samples,<sup>22</sup> and clearly more investigations are needed. However, the observation of hole transits in the TOF experiment, with a  $\mu\tau$  product of  $10^{-7} \text{cm}^2/\text{V}$ ,<sup>2</sup> also implies that the density of deep trapping states below the Fermi energy cannot be greater than about  $10^{15} \text{cm}^{-3}$ , given the known capture cross sections.<sup>2,23</sup>

To summarize the results of this section, one can identify a regime in which the sample is fully depleted of shallow states by a voltage pulse. The drift mobility and  $\mu\tau$  can be measured in the usual way with only a minor distortion of the internal field, but the voltage-pulse sweep out also gives very directly the density of shallow states as well as the bulk conductivity of the sample. This regime

can be recognized by a sweep out charge that is independent of voltage, and with a decay time constant inversely proportional to  $V$ . We also note that complete depletion can be achieved in highly doped *n*-type samples provided the layer thickness is sufficiently small. These results using samples in which a thin *n*-type layer is sandwiched between undoped *a*-Si:H are reported elsewhere.<sup>18</sup>

#### IV. GAP-CELL PHOTOCONDUCTIVITY

The usual analysis of TOF data assumes that the sample is a perfect capacitor. However, the results described above highlight the fact that *n*-type samples do not meet this approximation, and instead act as a depletion-layer capacitance and a series resistance. As a result the transient-photoconductivity data contains no information about bulk transport and recombination. In the same way the assumption that a gap cell is a perfect resistor is incorrect since there is again the depletion-layer capacitance in series. A qualitatively similar transient response in the two types of samples seems likely. It is therefore a reasonable expectation that some aspects of the transient-photoconductivity decay of gap-cell structures may be related to contact and space-charge effects rather than bulk transport and recombination.

It is usually argued that such contact effects are absent in gap cells because the applied voltage is typically large and the gap is wide. The earlier example of a leakage current of  $10^{-8}$  A/cm<sup>2</sup> and a bulk resistivity of  $10^{10}$  Ω cm results in a voltage drop of 10 V for a gap of 1 mm compared with 50 mV for a sandwich cell of thickness 5 μm. In addition the leakage current is probably larger in the gap cell because of fringing field effects. Hence the resistor approximation may be reasonable for undoped *a*-Si:H in the dark. However, the dark conductivity of *n*-type samples and the photoconductivity of undoped are typically 3–5 orders of magnitude larger, resulting in a much smaller bulk voltage drop compared to that at the contact.

If contact effects are present, they are likely to be more apparent in doped samples because these have a lower series resistance and larger depletion layer capacitance than undoped *a*-Si:H. Our measurements have been made on a variety of doped and undoped samples, and are illustrated with results using a doping level of  $3 \times 10^{-5}$  PH<sub>3</sub>/SiH<sub>4</sub>, with an electrode spacing of 1 mm.

Figures 12 and 13 show a summary of typical data. Figure 12 illustrates the transient-photocurrent decay at different dc voltages, on a  $\log I$  versus  $\log t$  plot. At low voltages the decay extends over a moderately broad time scale with a mean decay (defined where the slope of the data is  $-1$ ) of about  $10^{-4}$  sec. At high voltages the initial decay is similar but there is also a slowly decaying tail whose relative intensity increases with applied voltage. As shown in the extended data of Fig. 13, the tail continues for at least 1 sec.

Figure 12 also shows the transient photoresponse at zero bias when one of the electrodes is shielded from the excitation light. A substantial photocurrent is observed with a decay that is very similar to the low-voltage data. When both electrodes are exposed at zero bias, the resulting photocurrent depends on the alignment of the excita-

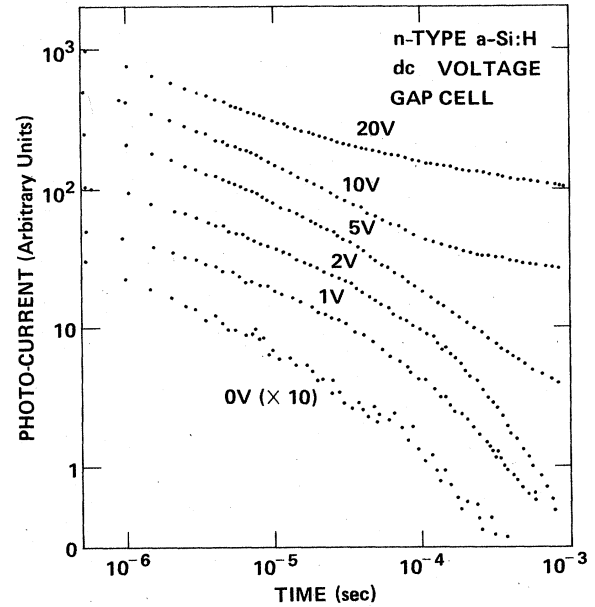


FIG. 12. Examples of the photocurrent decay in the *n*-type gap-cell sample, at different dc voltages. The results at zero bias are with one electrode shielded.

tion light. The laser beam has a diameter of about 5 mm and so completely fills the gap. However, if the beam is offset towards one electrode, a zero-bias response is observed, which changes sign as the beam is offset towards the other electrode. When the beam is symmetrical in the gap (as it is for all the other data), no zero-bias response is observed.

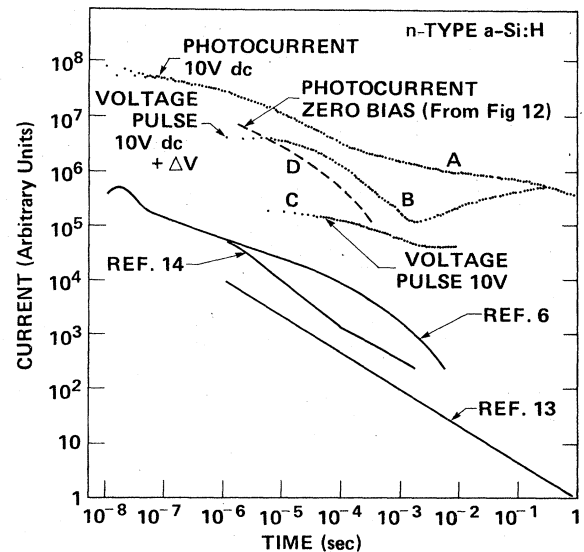


FIG. 13. An example of the photocurrent decay over an extended time range in the *n*-type sample (curve A). Also shown are the voltage-pulse responses as described in the text (curves B and C). The dashed curve (D) is the zero-bias decay taken from Fig. 12 for comparison. Solid lines are some published photoconductivity data.

In addition to the extended photocurrent transient, Fig. 13 shows voltage-pulse data. A simple voltage pulse (curve *B*) exhibits an initial transient current which appears to reach steady state after about  $10^{-3}$  sec. The initial current is typically 3 times larger than the steady-state value. In fact a true steady state is not reached until much longer times as the current rises slowly. This is more easily seen in the other voltage-pulse data in Fig. 13 (curve *C*). For these data a small voltage step ( $\sim 0.1$  V) is added to a 10-V-dc background. In addition, for clarity, a constant current has been subtracted. This makes it easier to see the initial decrease in current being followed by the slow increase that extends for at least 1 sec.

#### A. Analysis

The discussion begins by focusing on the portion of the transient response that extends up to  $10^{-4}$ – $10^{-3}$  sec. An initial observation is that the zero-bias response *must* originate from a contact effect. The bulk of the sample has no longitudinal electric field, and any diffusion must be symmetrical. In addition the sign of the response depends only on which contact is illuminated more strongly. Near each contact there is a depletion layer down which the photoexcited electrons will drift. The depletion-layer width is no more than  $1 \mu\text{m}$ , so that the maximum charge collection due to the electrostatic term, as defined in Sec. III A, is  $10^{-3}$  times the number of electrons generated in the depletion layer, which can only be  $10^{-3}$  times the total illumination of the 1-mm gap. The measured charge is much larger than this quantity, and in addition the decay time is very much greater than the drift time across such a thin depletion layer. Evidently the transient response is dominated by the screening term, as was observed in sandwich cells, and which is expected to dominate under conditions of a narrow depletion width  $w/d$  and a low-series resistance. The expected time constant for the decay is therefore the appropriate value of  $RC$ . For this particular sample the resistance  $R$  is about  $3 \times 10^5 \Omega$  and the depletion-layer capacitance is estimated to be of order 100 pf. These values give an estimated time constant of  $10^{-5}$ – $10^{-4}$ , in reasonable agreement with the observations. Hence the zero-bias response is consistent with expectations for a depletion-layer sweep-out effect.

The observation that the low-voltage data of Fig. 12 all have an almost identical time dependence as the zero-bias results leads us to conclude these results are also due to sweep out with the same  $RC$  time constant. Further justification for this explanation comes from the obvious analogy with the sandwich-cell results discussed before. In addition, if the interpretation is correct, comparable time constants should be observed in voltage-pulse data. Figure 13 confirms this expectation. In the voltage-pulse measurements the current decays with a time constant of  $\sim 10^{-4}$  sec, which is clearly due to sweep out of the depletion-layer charge. The fact that the steady-state current is about  $\frac{1}{3}$  of the initial value implies that  $\frac{2}{3}$  of the voltage is dropped across the contact and only  $\frac{1}{3}$  across the bulk.

It is unclear exactly what role the bulk photoconductivity plays in these results. At nonzero voltages there is a bulk electric field and therefore there will be a bulk photo-

current. However, since the capacitance of the gap is very small, the photocurrent inevitably leads to a space-charge buildup near an electrode with a consequent field redistribution that has the  $RC$  time constant of the depletion layer and series resistance. Hence although the magnitude of the photocurrent is no doubt related to the true bulk effect, its decay is entirely dominated by the  $RC$  time constant and has no direct connection with the bulk recombination time or to any bulk transport property.

The slow photocurrent decay occurring at times longer than  $10^{-3}$  sec evidently has a different origin, since it is too slow for the internal screening effect. Nevertheless there is clear evidence that this component is also contact related. The voltage-pulse data shows that the current changes on the same time scale. This effect can only be caused by an internal-field redistribution, and is readily explained by the shrinking of the depletion layer as electrons are emitted from deep states. The emission process is known to take greater than 1 sec,<sup>16</sup> as is also evident from the results of Fig. 7. Since these changes occur over times longer than the screening time constant, the bulk current  $I_B$  must equal the leakage current at the contact  $I_C$ . These quantities are given by

$$I_B = \sigma E_B \quad (10)$$

and

$$I_C = f(E_C), \quad (11)$$

where  $\sigma$  and  $E_B$  are the bulk conductivity and field, and  $f$  is a nonlinear function of the contact field  $E_C$  and corresponds to the reverse-bias leakage of the Schottky contact. In addition the voltage drop is divided between the contact and the bulk,

$$V = V_C + V_B = E_C w + E_B d, \quad (12)$$

where  $w$  is the effective depletion-layer width. The emission of electrons from deep states increases the space charge in the depletion layer and from Poisson's equation, together with Eq. (12), this charge could either be manifested as a reduction in  $w$  and  $V_C$  or by an increase in  $E_C$ , and therefore also of  $I_C$ . In practice, both effects must occur since a larger  $I_C$  must be balanced by an equal increase in  $I_B$ , which can only be obtained by a larger voltage drop across the bulk, and hence a smaller  $V_C$ . Thus the slow increase in current is explained by the slow equilibration of the contact layer. A similar slow increase of the leakage current has also been observed in sandwich samples.<sup>18</sup>

Our interpretation of the slow photocurrent decay is based on a similar mechanism. Illumination increases  $\sigma$  and therefore  $I_B$ , so that the leakage current must increase to reach a steady state. The mechanism by which this occurs is the accumulation of positive space charge at the contact which is the inevitable consequence when  $I_C < I_B$ . As a result the depletion layer contracts and  $E_C$  increases until  $I_C$  and  $I_B$  are again equal.

When the light is turned off,  $\sigma$  returns to its dark value by recombination. The bulk current decays with a time constant governed by the internal  $RC$  time constant, as

discussed above, and the leakage current returns to equilibrium as the positive space charge at the contact is removed. If this last process is very slow, then the contact is capable of injecting more current than the bulk needs and in effect would change temporarily from being a blocking contact to being space-charge limited. There would be a higher current associated with the contact which would persist until the blocking nature of the contact is restored.

This effect is qualitatively the same as one studied earlier in which  $n^+$ -injecting contacts were used in a sandwich cell.<sup>9</sup> A transient photocurrent was observed to extend out to at least  $10^{-1}$  sec. The interpretation of this result was that trapped space charge at the contact caused an increase in the injection current, and that the space charge had a very long time constant for neutralization. Another similar situation is also discussed elsewhere.<sup>11</sup>

A complete analysis of the contact effect is extremely complicated, since it combines a detailed knowledge of the contact leakage, the depletion-layer profile, and the bulk transport. The present discussion is limited to arguing that the observed decay is consistent with our model. The neutralization of the positive space charge could occur by capture of electrons or release of holes. Certainly the release time of holes from dangling bonds is expected to be at least as large as for electrons and therefore  $\sim 1$  sec or more. We give two arguments as to why the equilibration time by the capture of electrons might also be very slow. First, the recombination time  $\tau$  for the capture of excess electrons is given by

$$\tau^{-1} = bn, \quad (13)$$

where  $n$  is the density of conduction-band electrons and  $b$  is the recombination coefficient for trapping into the deep states that comprise the space charge. The current is related to the local field by

$$I = ne\mu E. \quad (14)$$

If the field  $E(x)$  varies spatially in the sample, then the recombination time also varies and at any point is given, from Eqs. (13) and (14), by

$$\tau(x) = e\mu E(x)/Ib. \quad (15)$$

Hence the recombination time is proportional to the field  $E$ . Since the field has its maximum value near the electrode because of the depletion layer, the neutralization of positive space charge will be particularly slow, and can be several orders of magnitude longer than the bulk recombination time. The point is that because the field is large, the density of electrons is very low, giving a long recombination time.

The second argument is even more elementary. The steady-state depletion layer at the contact is maintained by a dynamic equilibrium between the capture of electrons into deep traps, and their release. As equilibrium is approached these rates must be equal. Hence the time constant is given approximately by the electron emission time.

## B. Discussion

Our data show that, at least for some specific experimental conditions, the transient photoconductivity decay is entirely determined by an internal  $RC$  time constant, and a slow space-charge equilibration at the contact. It is pertinent to ask whether other published data are dominated by the same effects. The experimental situation is very complicated because the magnitude of the contact effect depends on the nature of the metal contact, the sample conductivity, the sample geometry, as well as the particular voltage and light intensity used. Nevertheless, Fig. 13 shows some reported decay data on undoped and  $n$ -type *a*-Si:H (including our own) which show a distinct resemblance to our present results. We believe that in the absence of proof to the contrary, these results must be attributed to the contact artifacts.

It should be emphasized that the contact problem is much less significant in measurements of steady-state photoconductivity. Here the error is only in the absolute magnitude of the deduced conductivity, which occurs because some of the voltage is dropped at the contact. The error may be as large as a factor 2–5, but is unlikely to be any greater, and probably does not affect the qualitative results of an experiment. On the other hand, the apparent decay time can be many orders of magnitude larger than the real recombination time.

One can also ask whether a structure can be designed in which these effects do not exist. We believe that this is not possible using a two-terminal device with any metal contact that forms a depletion layer. Certainly the relative voltage drop across the bulk can be enhanced by using a high voltage and a wide gap, but then the space-charge accumulation may be larger and the gap capacitance is smaller. An alternative is to use Ohmic (e.g.,  $n^+$ ) contacts. However, under conditions of space-charge limited injection, similar decay artifacts are observed.<sup>9,11</sup> Possibly, very low voltages, avoiding injection, may eliminate the problem. However, even if the contact effects can be eliminated, other artifacts can influence the transient decay of photoconductivity. One example is the result of surface band bending, as described elsewhere.<sup>24</sup> Certainly the measurement and interpretation of gap-cell photoconductivity must be approached with great caution.

## V. CONCLUSIONS

These results show that in doped *a*-Si:H samples of sufficient bulk conductivity, the uniform-field approximation invariably breaks down, and the TOF data give little or no information about the drift mobility of carrier lifetime. For our own sample deposition conditions, this regime occurs at a doping level of 1 ppm in  $n$ -type samples, and above 100 ppm in  $p$ -type. The transient response of doped samples is governed by the depletion-layer capacitance and the bulk-series resistance. Two different conditions can be identified depending on whether or not a voltage pulse completely depletes the sample. In either case the results can be analyzed to obtain the density of shallow occupied states in the band tails. Both  $n$ - and  $p$ -type samples have been measured, and the occupied tail-state density is found to be as low as  $10^{14}$  cm<sup>-3</sup>. TOF mea-

surements with a variable delay after the voltage pulse allows one to study the shrinking of the depletion layer as carriers are emitted from deep states.

Results of transient conductivity and photoconductivity from gap-cell samples are also presented. The response is found to have similar characteristics as for doped sandwich-cell structures. It is deduced that these data are also determined by the depletion-layer capacitance and series bulk resistance, with an additional very slow decay attributed to the shrinking of the depletion layer by emis-

sion from deep states. It is suggested that some transient-photoconductivity decay data may have been mistakenly interpreted.

#### ACKNOWLEDGMENTS

The author is grateful to M. Thompson for providing samples and to J. Zesch for expert technical assistance. The work is supported by the Solar Energy Research Institute (Golden, CO).

- 
- <sup>1</sup>G. Pfister and H. Scher, *Adv. Phys.* **27**, 747 (1978).  
<sup>2</sup>R. A. Street, M. J. Thompson, and J. Zesch, *Appl. Phys. Lett.* **43**, 672 (1983).  
<sup>3</sup>W. E. Spear, H. L. Steemers, P. G. Le Comber, and R. A. Gibson, *Philos. Mag.* **B 50**, L33 (1984).  
<sup>4</sup>P. B. Kirby and W. Paul, *Phys. Rev. B* **29**, 826 (1984).  
<sup>5</sup>T. Tiedje and A. Rose, *Solid State Commun.* **37**, 49 (1980).  
<sup>6</sup>J. M. Hvam and M. H. Brodsky, *Phys. Rev. Lett.* **46**, 371 (1981).  
<sup>7</sup>T. Tiedje, J. M. Cebulka, D. L. Morel, and B. Abeles, *Phys. Rev. Lett.* **21**, 1425 (1981).  
<sup>8</sup>C.-Y. Huang, S. Guha, and S. J. Hudgens, *Phys. Rev. B* **27**, 7460 (1983).  
<sup>9</sup>R. A. Street, *Phys. Rev. B* **27**, 4924 (1983).  
<sup>10</sup>T. Datta and M. Silver, *Appl. Phys. Lett.* **38**, 903 (1981).  
<sup>11</sup>R. A. Street, M. J. Thompson, and N. M. Johnson, *Philos. Mag.* **B 51**, 1 (1985).  
<sup>12</sup>R. A. Street and M. J. Thompson, *Appl. Phys. Lett.* **45**, 769 (1984).  
<sup>13</sup>R. A. Street, *Solid State Commun.* **39**, 263 (1981).  
<sup>14</sup>N. Matsumoto, T. Kagawa, G. Motosugi, and K. Kumabe, *Jpn. J. Appl. Phys.* **2**, Suppl. 20, 179 (1981).  
<sup>15</sup>See, for example, A. Rose, *Concepts in Photoconductivity and Allied Problems* (Wiley, New York, 1963).  
<sup>16</sup>N. M. Johnson, *Appl. Phys. Lett.* **42**, 981 (1983).  
<sup>17</sup>D. V. Lang, J. D. Cohen, and J. P. Harbison, *Phys. Rev. B* **25**, 5285 (1982).  
<sup>18</sup>R. A. Street, *Philos. Mag.* **B 50**, L19 (1984).  
<sup>19</sup>T. Tiedje, in *The Physics of Hydrogenated Amorphous Silicon II*, Vol. 56 of *Topics in Applied Physics*, edited by J. D. Joannopoulos and G. Lucovsky (Springer, New York, 1984), Chap. 6.  
<sup>20</sup>R. A. Street, D. K. Biegelsen, and J. C. Knights, *Phys. Rev. B* **24**, 969 (1981).  
<sup>21</sup>W. B. Jackson and N. M. Amer, *Phys. Rev. B* **25**, 5559 (1982).  
<sup>22</sup>H. Dersch, J. Stuke, and J. Beichler, *Phys. Status Solidi B* **105**, 265 (1981).  
<sup>23</sup>R. A. Street, *Philos. Mag.* **B 49**, L15 (1984).  
<sup>24</sup>W. B. Jackson, R. A. Street, and M. J. Thompson, *Solid State Commun.* **47**, 435 (1983).